

2022

## Probing the Effect of Hyperglycemia on Endothelial Force Generation and Transmission

Jovani J. Gutierrez  
*University of Central Florida*

 Part of the [Biomechanics and Biotransport Commons](#), and the [Mechanical Engineering Commons](#)

Find similar works at: <https://stars.library.ucf.edu/honorsthesis>

University of Central Florida Libraries <http://library.ucf.edu>

This Open Access is brought to you for free and open access by the UCF Theses and Dissertations at STARS. It has been accepted for inclusion in Honors Undergraduate Theses by an authorized administrator of STARS. For more information, please contact [STARS@ucf.edu](mailto:STARS@ucf.edu).

---

### Recommended Citation

Gutierrez, Jovani J., "Probing the Effect of Hyperglycemia on Endothelial Force Generation and Transmission" (2022). *Honors Undergraduate Theses*. 1242.  
<https://stars.library.ucf.edu/honorsthesis/1242>

PROBING THE EFFECTS OF HYPERGLYCEMIA ON ENDOTHELIAL  
FORCE GENERATION AND TRANSMISSION

by

JOVANI JOELLE GUTIERREZ

A thesis submitted in partial fulfillment of the requirements  
for the Honors in the Major Program in Mechanical Engineering  
in the College of Engineering and Computer Science  
and in the Burnett Honors College  
at the University of Central Florida  
Orlando, Florida

Summer Term  
2022

## **ABSTRACT**

This thesis intends to utilize biomechanics to study the endothelial biomechanical response in a static hyperglycemic microenvironment. Hyperglycemia is a diabetic condition with abnormally high levels of glucose in the bloodstream. The effects of hyperglycemia over time lead to vascular complications resulting in patients being more prone to cardiovascular diseases. Current studies have focused on the molecular mechanisms affected by hyperglycemia; however, the mechanical mechanisms by which hyperglycemia causes vascular structural and functional changes are understudied. Therefore, to study the effects of hyperglycemia in the endothelium, Human Umbilical Vein Endothelial Cells (HUVEC) were cultured under three glucose conditions: normal glucose (4 mmol/l D-glucose), high glucose (30 mmol/l D-glucose), and an osmotic control (4 mmol/l D-glucose + 26 mmol/l D-mannitol). To evaluate the biomechanical response, we used traction force microscopy and monolayer stress microscopy to measure the cell-substrate tractions and cell-cell intercellular stresses. For the RMS tractions, HUVEC monolayers exposed to high glucose decreased by 10%, while the osmotic control decreased by 17% compared to the normal glucose. HUVEC monolayers exposed to high glucose produced average normal stresses that were 53% lower than monolayers exposed to normal glucose, while the osmotic control decreased by 51% compared to the normal glucose. For the maximum shear stresses, HUVEC monolayers exposed to high glucose decreased by 20%, while the osmotic control decreased by 14% compared to the normal glucose. To conclude this study, we report that hyperglycemia lowers the biomechanical response in the endothelium compared to normal glucose conditions. These results will contribute to understanding the specific role hyperglycemia has on endothelial mechanics and its role in the progression and development of cardiovascular diseases in diabetic patients.

## TABLE OF CONTENTS

|                                |    |
|--------------------------------|----|
| Abstract.....                  | ii |
| List of Figures.....           | iv |
| Background and Motivation..... | 2  |
| Materials and Methods.....     | 3  |
| Results and Discussion.....    | 7  |
| Conclusion.....                | 14 |
| References.....                | 16 |

## LIST OF FIGURES

Figure 1: Schematic of Endothelial Cells within Blood Vessel ..... 4

Figure 2: Schematic of Traction and Normal/Shear Intercellular Stresses ..... 6

Figure 3: Phase contrast images of HUVEC monolayers treated with different levels of glucose. Phase contrast images of normal glucose treated HUVECS at 0 hours (a), 1.5 hours (b), and 3 hours (c). Phase contrast images of osmotic control treated HUVECS at 0 hours (d), 1.5 hours (e), and 3 hours (f). Phase contrast images of high glucose treated HUVECS at 0 hours (g), 1.5 hours (h), and 3 hours (i). Scale bar represents entire image which is 500 x 500  $\mu\text{m}$ . ..... 7

Figure 4: HUVEC monolayers exposed to high glucose decreased by 53% in magnitude for average normal intercellular stresses compared to normal glucose conditions after 3 hours. HUVEC monolayers exposed to the osmotic control decreased by 51% in magnitude compared to the normal glucose after the 3 hours. Average normal intercellular stresses (Pa) of HUVEC monolayers treated with different levels of glucose are shown in this figure. The figure labels show the average normal intercellular stresses for normal glucose treated HUVEC at 0 hour (a), 1.5 hours (b), and 3 hours (c), osmotic control treated HUVEC at 0 hour (d), 1.5 hours (e), and 3 hours (f), and high glucose treated HUVEC at 0 hour (g), 1.5 hours (h), and 3 hours (i). Scale bar represents the entire image which is 500 x 500  $\mu\text{m}$ . ..... 9

Figure 5: HUVEC monolayers exposed to high glucose decreased by 20% in magnitude for maximum shear intercellular stresses compared to normal glucose conditions after 3 hours. HUVEC monolayers exposed to the osmotic control decreased by 14% in magnitude compared to the normal glucose after the 3 hours. Maximum Shear Intercellular Stresses (Pa) of HUVEC monolayers treated with different levels of glucose are shown in this figure. The figure labels show the maximum shear intercellular stresses for normal glucose treated HUVEC at 0 hour (a), 1.5 hours (b), and 3 hours (c), osmotic control treated HUVEC at 0 hour (d), 1.5 hours (e), and 3 hours (f), and high glucose treated HUVEC at 0 hour (g), 1.5 hours (h), and 3 hours (i). Scale bar represents the entire image which is 500 x 500  $\mu\text{m}$ . ..... 10

Figure 6: High Glucose and Osmotic Control conditions showcased decreased average normal stresses and maximum shear stresses compared to normal glucose conditions over the course of 3 hours. This figure shows a comparison of the Average Normal Intercellular Stress (Pa) (figure 6.A) and Maximum Shear Intercellular Stress (Pa) (figure 6.B) of HUVEC monolayers in different glucose conditions over time. Error bars represented standard error. .... 11

Figure 7: HUVEC monolayers exposed to high glucose decreased by 10% in magnitude for RMS tractions compared to normal glucose conditions after 3 hours. HUVEC monolayers exposed to the osmotic control decreased by 17% in magnitude compared to the normal glucose after the 3 hours. RMS Traction (Pa) distributions of HUVEC monolayers with different glucose conditions are shown in this figure. The figure labels show the RMS tractions for normal glucose treated HUVEC at 0 hour (a), 1.5 hours (b), and 3 hours (c), osmotic control treated HUVEC at 0 hour (d), 1.5 hours (e), and 3 hours (f), and high glucose treated HUVEC at 0 hour (g), 1.5 hours (h), and 3 hours (i). Scale bar represents the entire image which is 500 x 500  $\mu\text{m}$ . ..... 12

## **BACKGROUND AND MOTIVATION**

According to the CDC, Diabetes Mellitus affects over 37.3 million individuals in the United States, which correlates to 11.3% of the population being affected [1]. Diabetes Mellitus is a metabolic condition in which the body has complications regulating the hormone insulin, causing blood glucose to spike to abnormally high levels. The American Diabetes Association has stated that cardiovascular diseases are the number one cause of death in people living with diabetes because diabetic patients are twice more likely to develop the disease [2].

The technical term for abnormally high blood glucose levels from diabetes is hyperglycemia. Hyperglycemia is when too much glucose is in the body because the body has complications regulating insulin. Hyperglycemia is a blood glucose level greater than ten millimoles per liter (mmol/l), while normal glucose levels range from 4 to 7.8 millimoles per liter (mmol/l) [3].

Studies have shown that hyperglycemia increases the extracellular osmotic pressure causing hyperosmolarity [4]. The abundance of the glucose molecule in the bloodstream leads to water being pulled out of the cells. This leads to the extra glucose molecule being passed into urine, which increases urination and dehydration [4]. When dehydration occurs, the kidney can no longer get rid of the excess glucose resulting in the glucose level in your blood becoming excessively high. The loss of water makes the blood concentration extremely concentrated and causes impairments to water movement within other body organs. This is known as diabetic hyperglycemic hyperosmolar syndrome, occurring at a blood glucose concentration above 33.3 millimoles per liter (mmol/l) [5]. Since hyperglycemia is a hypertonic solution, we must control the osmotic pressure using D-mannitol, which will act as an osmotic control. D-

mannitol molecule is an osmotic diuretic agent that prevents the reabsorption of water and sodium [6].

Hyperglycemia, insulin-resistivity, obesity, and other metabolic disorders are some of the significant factors of diabetes that may lead to the progression of cardiovascular diseases [7]. The specific role that hyperglycemia plays in endothelial dysfunction and cardiovascular diseases is difficult to define because many factors influence the progression of the disease. Hyperglycemia has been shown to induce oxidative stress, which deteriorates endothelial functions [8]. Oxidative stress concerns the balance between the production and accumulations of reactive oxygen species (ROS). Multiple studies have showcased that hyperglycemia and diabetes reduce the amount of nitric oxide (NO) available by affecting the NO production in endothelial cells by a surplus of ROS scavenging NO [9]. When the NO is low, endothelial cells begin to lose their function of controlling vascular tone [9]. ROS play a critical role in several cardiovascular complications induced by hyperglycemia. ROS are essential to normal cell function by acting as signaling molecules, but undesired consequences may occur in high amounts. ROS affects the endothelium's ability to dilate, increases apoptosis, and contributes to atherosclerotic lesions by enhancing monocyte adhesions [9]. Hyperglycemia has also been found to have effects on the adherens junctions that bind endothelial cells together. Hyperglycemia disturbs these junctions by leading to the tyrosine phosphorylation of vascular endothelial cadherin through protein kinase C- $\beta$  and myosin light chain phosphorylation [10]. Hyperglycemia also increases the trans-endothelial migrations of leukocytes [10]. These are some of the molecular mechanics affected by hyperglycemia, but we are interested in

understanding the mechanical mechanisms involved and why the endothelium has impairments controlling vascular tone.

The study of the endothelial model has become a central issue for understanding the relationship between diabetes and cardiovascular diseases. Endothelial cells are the primary cell type found in the inside lining of blood vessels, as shown in Figure 1. They have an anti-coagulant surface and are responsible for performing multiple critical physiological functions. These cells maintain cardiovascular homeostasis through vascular tone, permeability regulation, inflammation, injury repair, and the growth and regression of blood vessels [11-13].

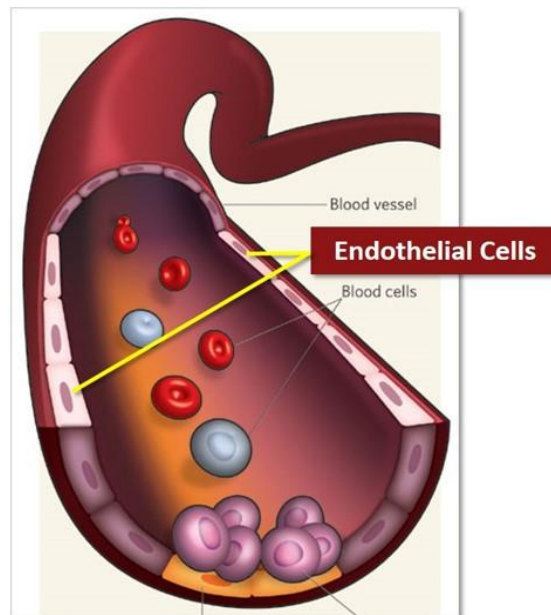


Figure 1: Schematic of Endothelial Cells within Blood Vessel [17]

Endothelial Cells in high glucose are dysfunctional. High glucose causes increased permeability in endothelial cells allowing solutes to pass through the vascular wall more frequently. This leads to more inflammation, giving individuals a higher risk for vascular



complications. Elevated glucose levels also affect the production and response to vasodilates, such as NO affecting vascular tone. These two dysfunctions can lead to a decline in migration, proliferation, survival, wound healing, and angiogenesis in endothelial cells [14-16]. Altered glucose conditions and long-time exposure to these conditions play a central role in the progression and pathogenesis of cardiovascular complications surrounding hyperglycemia and diabetes. Current studies have analyzed how hyperglycemia affects the molecular mechanisms within the endothelium; however, the influence of hyperglycemia on the mechanical mechanisms affected such as endothelial force generation and transmission is yet to be examined.

Therefore, my objective for this project is to analyze and measure the tractions and intercellular stresses produced by Human Umbilical Vein Endothelial Cells monolayers under the influence of normal and high glucose conditions. We conducted experiments by culturing HUVEC monolayers with normal glucose (4 mmol/l of d-glucose), high glucose (30 mmol/l of D-glucose), and an osmotic control (4 mmol/l of D-glucose + 26 mmol/l of D-mannitol). Cells were seeded onto a micropatterned soft substrate with a stiffness of  $E = 1.2$  kPa and allowed to grow in standard media for 24 hours for a confluent circular monolayer. After 24 hours, cells were cultured in their respective media with different glucose treatments for an additional 24 hours. The tractions and intercellular stresses were measured using traction force microscopy and monolayer stress microscopy techniques. In this thesis, we present a distinct report of the endothelial biomechanical responses under different levels of glucose conditions. This report has the potential to contribute to a greater understanding of vascular biology and how hyperglycemia may lead and contribute to endothelial dysfunctions in diabetic patients.

## MATERIALS AND METHODS

### *Cell Culture*

Primary Human Umbilical Vein Endothelial Cells (HUVECs) were purchased commercially from ThermoFisher and cultured in medium 200 (ThermoFisher) supplemented with large vessel endothelial supplement (ThermoFisher) on 0.1% gelatin (Sigma-Aldrich) coated flasks at 37°C and 5% CO<sub>2</sub>. HUVEC were grown in standard media until 90-95% confluency before cellular micropatterning and glucose treatment. HUVEC at passage six was used for all experiments.

### *Polyacrylamide Gel Fabrication*

For static conditions, Polyacrylamide (PA) gels were created based on the protocol Steward et al. [18] on 35mm Petri dishes (Cellvis). The dishes will be treated with a bind silane solution for 45 mins and then air dried prior to gel polymerization. PA gel solution contains a mixture of ultra-pure water, 40% acrylamide (Bio-Rad), 2% bis-acrylamide (Bio-Rad), and 0.5  $\mu\text{m}$  diameter fluorescent, carboxylate-modified yellow-green microspheres beads (Invitrogen). The gel solution is then degassed for 45 mins. In addition, ammonium persulfate and TEMED (N, N, N', N'-tetramethylethane-1,2-diamine) are added to polymerize the gel on the treated petri dishes. Finally, with the help of 18mm glass coverslips, gels are flattened to yield a gel height of  $\sim 100 \mu\text{m}$  and stiffness of 1.2kPa. A stiffness of 1.2kPa is used as this stiffness closely mimics the stiffness of a healthy endothelium [18].

### *Cellular Micropattern Preparation*

Using the micropattern preparation protocol [18], a thin layer of polydimethylsiloxane (PDMS) (Dow Corning) is cured in a 100mm petri dish by mixing a solution of silicone base with a curing agent (20:1) overnight at room temperature. After fabrication, a circular PDMS section will be cut to the desired size, and small holes will be created using a 1.25 mm diameter biopsy punch. PDMS micropatterns are then placed on top of PA-gels, and patterned gels are then treated with sulfosuccinimidyl-6-(4-azido-2-nitrophenylamino) hexanoate (Sulfo-SANPAH; Proteochem) dissolved in 0.1 M HEPES buffer solution (Fisher Scientific) and placed under a UV lamp for 20 mins. After SANPAH burning, patterned gels are treated with 0.1 mg/ml of collagen-I (Advanced Biomatrix) overnight at 4°C. The following day, excess collagen is removed, and HUVECs are seeded and allowed to attach for 1 hour. After the hour concludes, micropatterns are removed, and HUVEC are allowed to form confluent monolayers in standard media 24 hours prior to glucose exposure.

### *Glucose Stimulation*

To begin experiments, HUVEC were cultured and incubated at 37°C in 5% CO<sub>2</sub> in standard medium and allowed to grow to 90-95% confluency in a T-25 flask. After HUVEC reached the desired confluency, the cells were then seeded into the circular micropatterns and allowed to reach full confluency for 24 hours in standard media. After the 24 hours, HUVEC were cultured in their respective glucose conditions with medium containing 4 mmol/l glucose (normal), 30 mmol/l glucose (high), or 4 mmol/l glucose + 26 mmol/l D-mannitol (osmotic control) for an additional 24 hours prior to experiments. Before taking the measurements,

HUVECs will be seeded in their appropriate plates and incubated with their respective glucose conditions for 3 hours on a Zeiss Inverted microscope.

### *Time Lapse Microscopy*

Utilizing a Zeiss inverted microscope with a 5X objective and Hamamatsu camera, phase contrast and fluorescent images were acquired every 5 minutes. During image processing, HUVEC monolayers will be supplemented in medium with their respective glucose treatment for 3 hours. For the last 10 mins, 10x trypsin will be added to disrupt the cells and detach them from the gel surface. This allows for a stress-free image of the gel's top surface to be obtained and used for traction force calculations.

### *Traction Force Microscopy (TFM) and Monolayer Stress Microscopy (MSM):*

Using a particle image velocimetry (PIV) routine in MATLAB, we can calculate the polyacrylamide gel's deformations produced by the cells to determine the cell displacements. This is done by comparing the raw stress-bead image to the reference or stress-free image taken at the end of the experiment. Using these displacements and Traction Force Microscopy (TFM), we can use Fourier Transform Traction Cytometry (FTTC) to calculate the cell-substrate forces [19]. These cell-to-substrate tractions are then balanced by the cell-to-cell intercellular stresses in a 2D plane. Using the cellular monolayer as boundary conditions, we mesh the entire monolayer region into small elements and perform a finite element analysis. By doing this, we can solve the equations to find the intercellular stresses and determine the principal stresses. By rotating the coordinate system by  $45^\circ$ , we compute the maximum principal stress ( $\sigma_{max}$ ) and minimum principal stresses ( $\sigma_{min}$ ) with their respective

orientations. At each section of the monolayer, we compute the average normal intercellular stress  $(\sigma_{\max} + \sigma_{\min})/2$  and maximum shear intercellular stress  $(\sigma_{\max} - \sigma_{\min})/2$  within the appropriate boundary conditions.

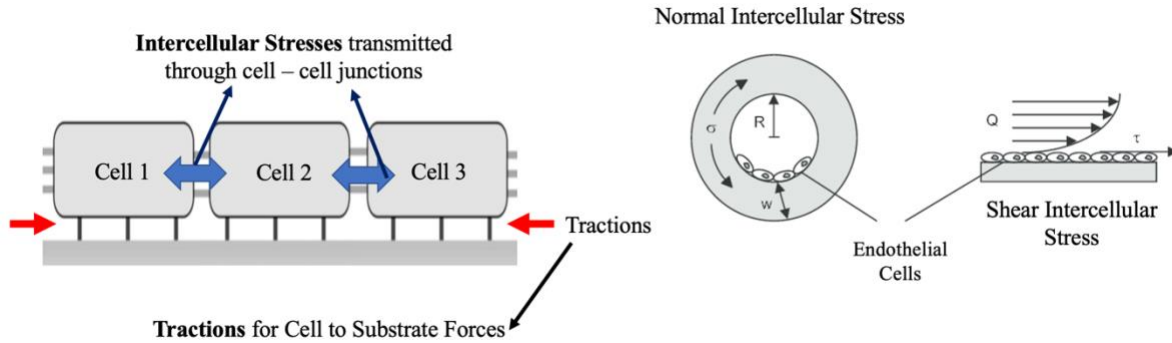


Figure 2: Schematic of Traction and Normal/Shear Intercellular Stresses [20]

### Statistics

The data was analyzed by an analysis of variance (ANOVA), and a 2-sample Student t-test was used to test for statistical significance using Excel. This experiment was conducted one time. A probability (P) value  $< 0.05$  was considered statistically significant and we used a sample size of (N=4) HUVEC monolayers for each respective glucose condition.

## RESULTS AND DISCUSSION

The results from all experiments were performed over a cropped 500 x 500  $\mu\text{m}$  section in the center of each micropatterned monolayer. Phase contrast images of normal glucose, osmotic control, and high glucose conditions at the beginning of the experiment (0 hours), halfway during the experiments (1.5 hours), and the end of the experiment (3 hours) are displayed in Figure 3 down below.

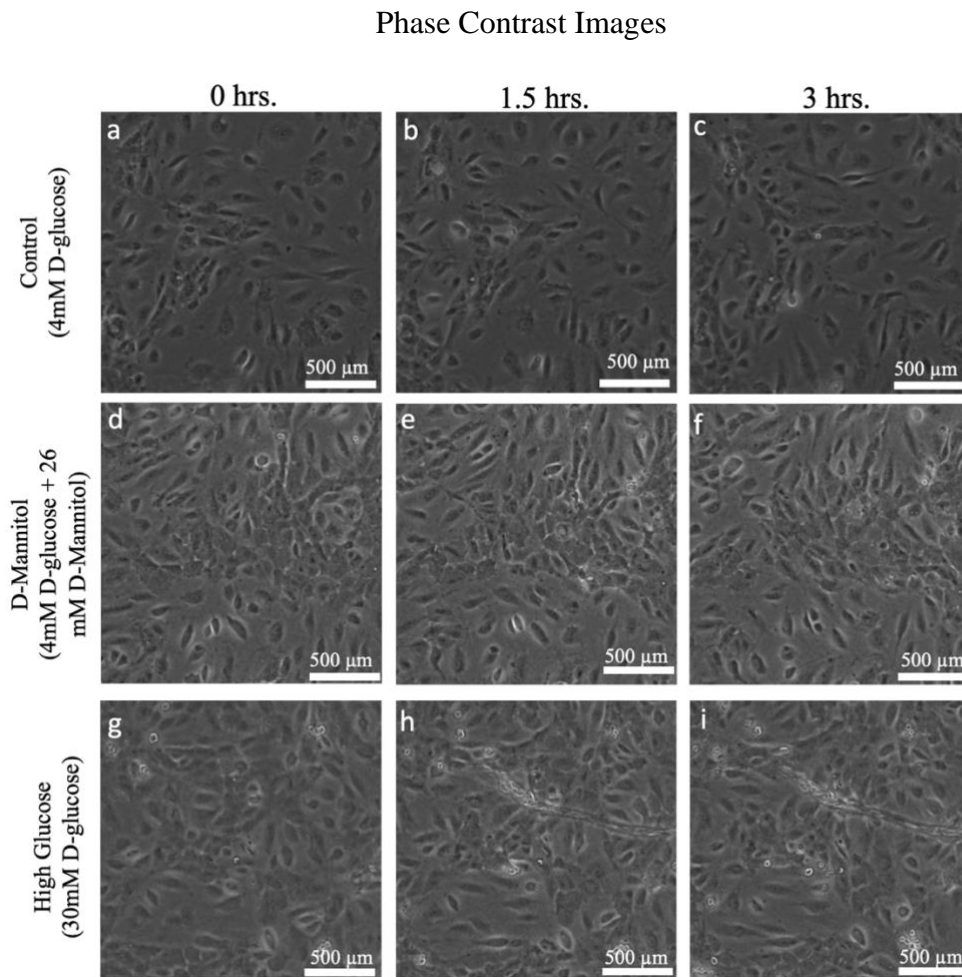


Figure 3: Phase contrast images of HUVEC monolayers treated with different levels of glucose. Phase contrast images of normal glucose treated HUVECS at 0 hours (a), 1.5 hours (b), and 3 hours (c). Phase contrast images of osmotic control treated HUVECS at 0 hours (d), 1.5 hours (e), and 3 hours (f). Phase contrast images of high

glucose treated HUVECS at 0 hours (g), 1.5 hours (h), and 3 hours (i). Scale bar represents entire image which is 500 x 500  $\mu\text{m}$ .

At the beginning of the experiment, average normal intercellular stresses were tensile and were  $60 \pm 20$  Pa for all glucose-treated conditions (Figure 4 a, d, and g). After one and half hours of the experiment, onset average normal intercellular stresses were  $118 \pm 7$  Pa,  $56 \pm 4$  Pa, and  $54 \pm 7$  Pa for normal, osmotic control, and high glucose conditions (Figure 4 b, e, and h). After 3 hours, the average normal intercellular stress was observed to be  $118 \pm 6$  Pa,  $57 \pm 4$  Pa, and  $55 \pm 5$  Pa for normal, osmotic control, and high glucose conditions, respectively (Figure 4 c, f, and i).

Average Normal Intercellular Stress (Pa)

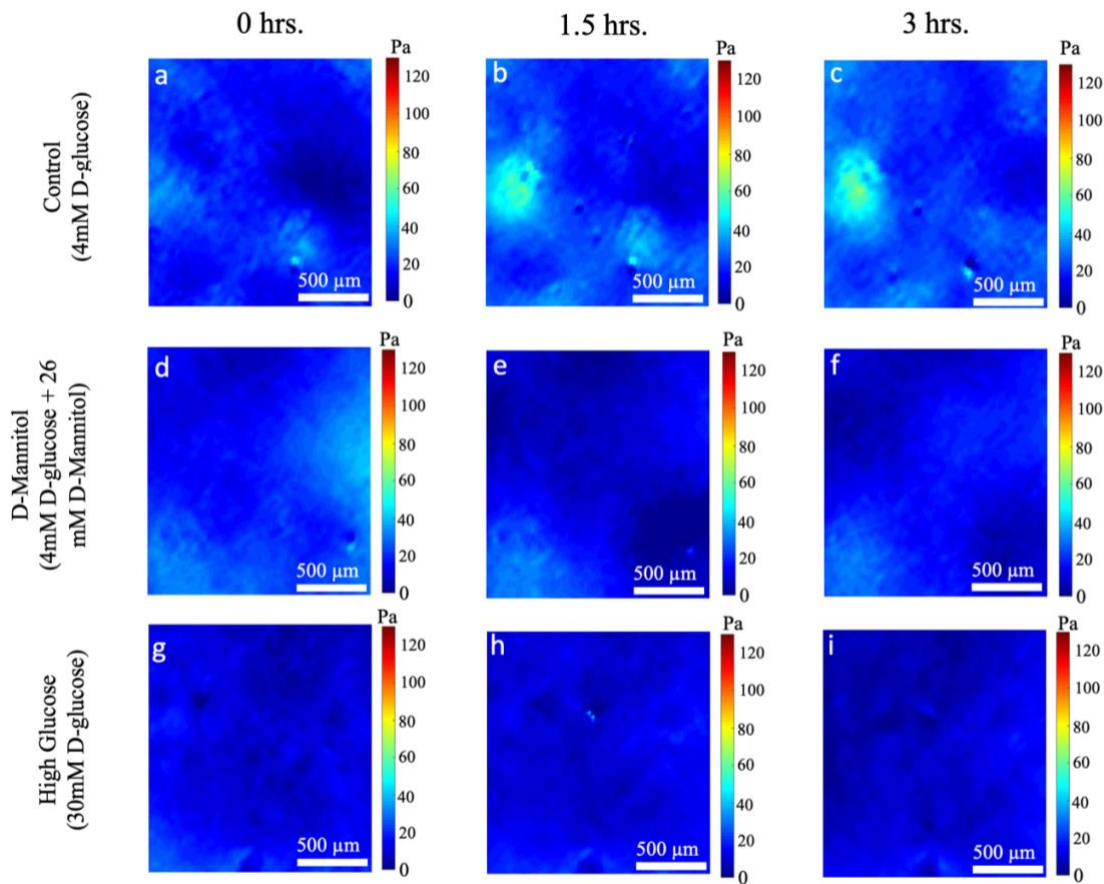


Figure 4: HUVEC monolayers exposed to high glucose decreased by 53% in magnitude for average normal intercellular stresses compared to normal glucose conditions after 3 hours. HUVEC monolayers exposed to the osmotic control decreased by 51% in magnitude compared to the normal glucose after the 3 hours. Average normal intercellular stresses (Pa) of HUVEC monolayers treated with different levels of glucose are shown in this figure. The figure labels show the average normal intercellular stresses for normal glucose treated HUVEC at 0 hour (a), 1.5 hours (b), and 3 hours (c), osmotic control treated HUVEC at 0 hour (d), 1.5 hours (e), and 3 hours (f), and high glucose treated HUVEC at 0 hour (g), 1.5 hours (h), and 3 hours (i). Scale bar represents the entire image which is 500 x 500  $\mu\text{m}$ .

At the initial time zero, the maximum shear intercellular stresses were tensile and were  $73 \pm 12$  Pa for all glucose treated conditions (Figure 5 a, d, and g). After one and half hours of the experiment, the maximum shear intercellular stresses were  $75 \pm 4$  Pa,  $63 \pm 3$  Pa, and  $57 \pm 5$  Pa at normal, osmotic control, and high glucose conditions (Figure 5 b, e, and h). After 3 hours, the maximum shear intercellular stresses were observed to be  $73 \pm 3$  Pa,  $63 \pm 2$  Pa, and  $58 \pm 4$  Pa for normal, osmotic control, and high glucose conditions, respectively (Figure 5 c, f, and i).



## Maximum Shear Intercellular Stress (Pa)

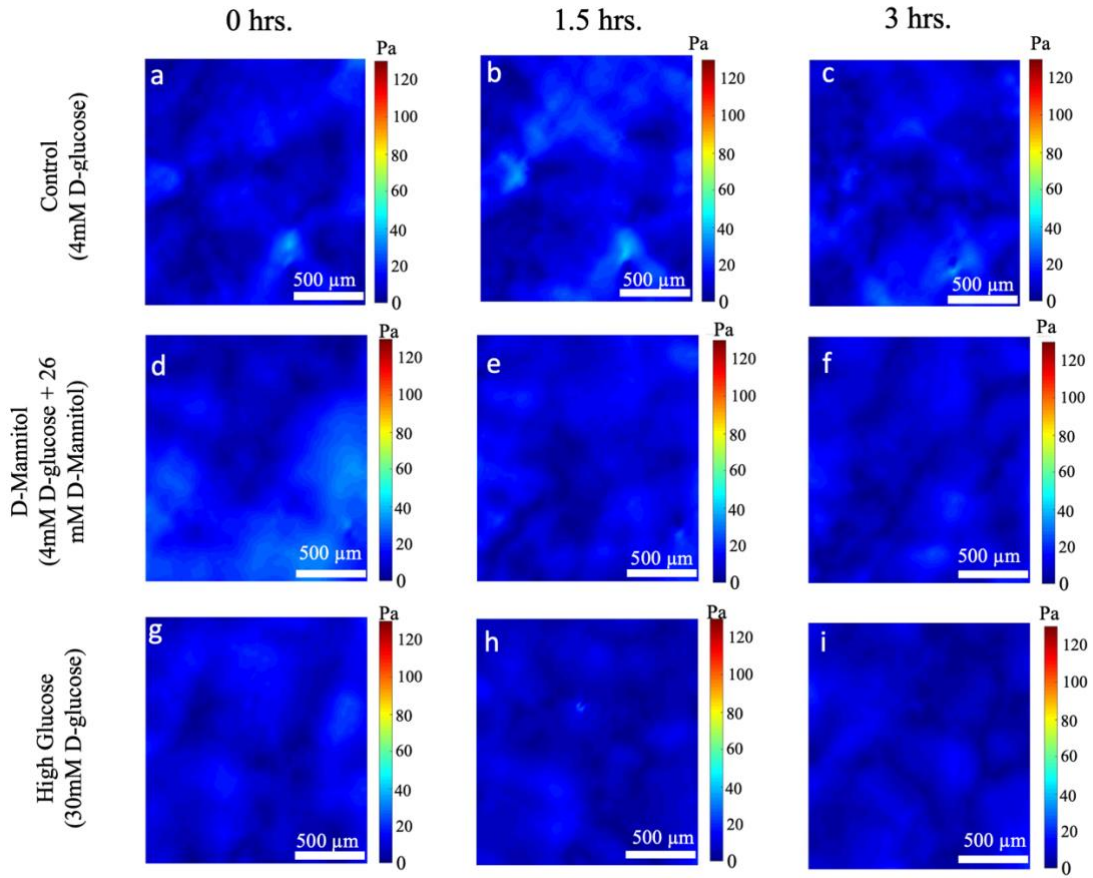


Figure 5: HUVEC monolayers exposed to high glucose decreased by 20% in magnitude for maximum shear intercellular stresses compared to normal glucose conditions after 3 hours. HUVEC monolayers exposed to the osmotic control decreased by 14% in magnitude compared to the normal glucose after the 3 hours. Maximum Shear Intercellular Stresses (Pa) of HUVEC monolayers treated with different levels of glucose are shown in this figure. The figure labels show the maximum shear intercellular stresses for normal glucose treated HUVEC at 0 hour (a), 1.5 hours (b), and 3 hours (c), osmotic control treated HUVEC at 0 hour (d), 1.5 hours (e), and 3 hours (f), and high glucose treated HUVEC at 0 hour (g), 1.5 hours (h), and 3 hours (i). Scale bar represents the entire image which is 500 x 500 μm.

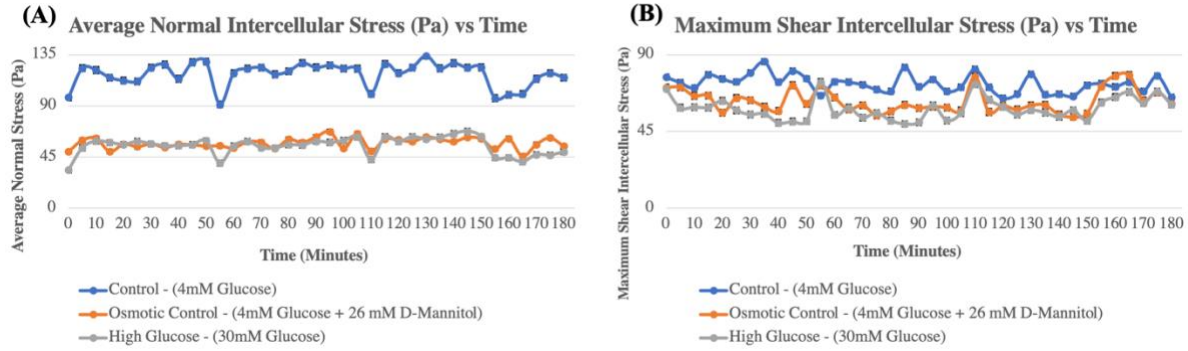


Figure 6: High Glucose and Osmotic Control conditions showcased decreased average normal stresses and maximum shear stresses compared to normal glucose conditions over the course of 3 hours. This figure shows a comparison of the Average Normal Intercellular Stress (Pa) (figure 6.A) and Maximum Shear Intercellular Stress (Pa) (figure 6.B) of HUVEC monolayers in different glucose conditions over time. Error bars represented standard error.

From Figure 6, we can observe a 65% and 53% decrease in magnitude of average normal intercellular stresses for HUVEC monolayers exposed to high glucose and a 49% and 51% decrease in magnitude of average normal intercellular stresses with osmotic control treated HUVEC monolayers when compared with normal glucose at 0 hours and 3 hours of experiment, respectively. At the same time, the maximum shear intercellular stresses decreased by 9% and 20% with HUVEC monolayers with high glucose and decreased again by 8% and 14% with HUVEC monolayers treated with D-mannitol compared to HUVEC with normal glucose at 0 hours and 3 hours, respectively.

## RMS Traction (Pa)

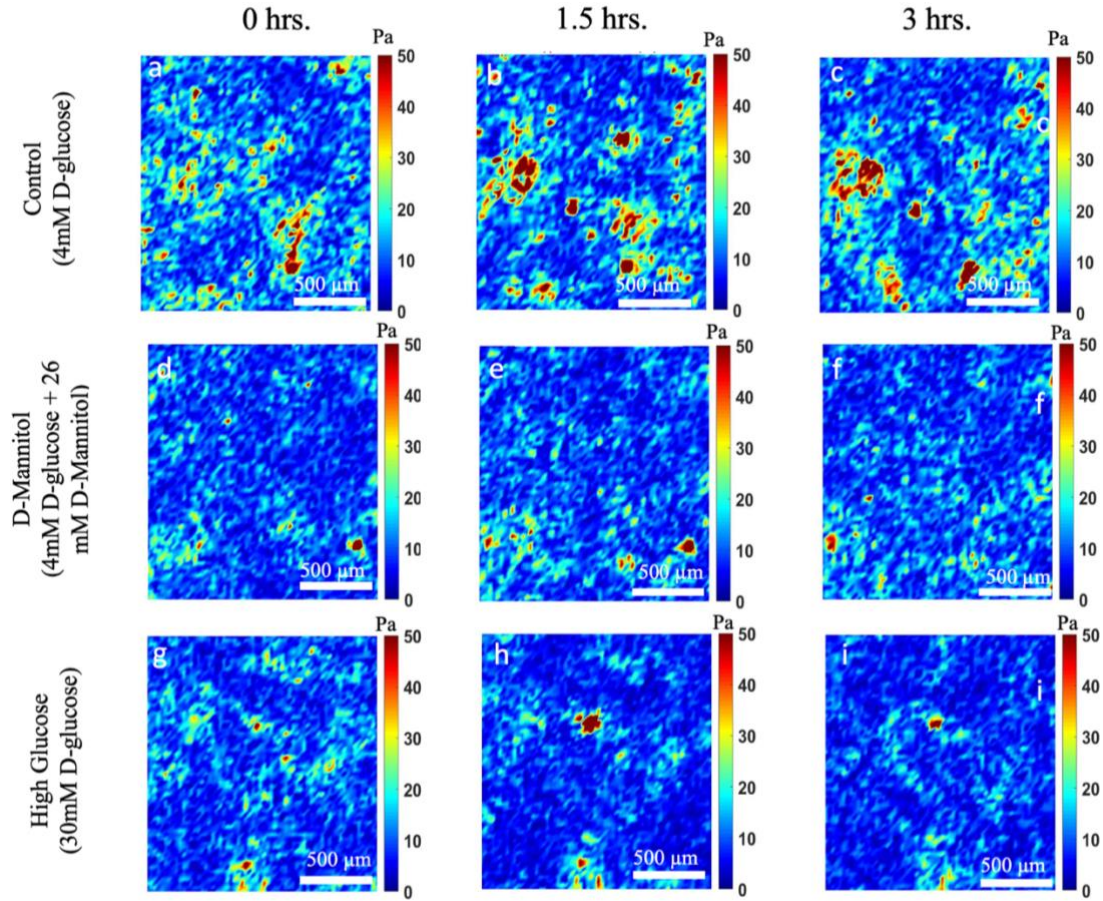


Figure 7: HUVEC monolayers exposed to high glucose decreased by 10% in magnitude for RMS tractions compared to normal glucose conditions after 3 hours. HUVEC monolayers exposed to the osmotic control decreased by 17% in magnitude compared to the normal glucose after the 3 hours. RMS Traction (Pa) distributions of HUVEC monolayers with different glucose conditions are shown in this figure. The figure labels show the RMS tractions for normal glucose treated HUVEC at 0 hour (a), 1.5 hours (b), and 3 hours (c), osmotic control treated HUVEC at 0 hour (d), 1.5 hours (e), and 3 hours (f), and high glucose treated HUVEC at 0 hour (g), 1.5 hours (h), and 3 hours (i). Scale bar represents the entire image which is 500 x 500 μm.

At the initial time zero, the RMS tractions were tensile and were  $11 \pm 0.7$  Pa for all glucose treated conditions (Figure 7 a, d, and g). After one and half hours of experiment, onset RMS tractions were  $12 \pm 0.3$  Pa,  $10 \pm 0.2$  Pa, and  $11 \pm 0.5$  Pa at normal, osmotic control, and high

glucose conditions (Figure 7 b, e, and h). After 3 hours, the RMS tractions was observed to be  $12 \pm 0.3$  Pa,  $10 \pm 0.2$  Pa, and  $11 \pm 0.4$  Pa for normal, osmotic control, and high glucose conditions, respectively (Figure 7 c, f, and i). This indicated a 14% and 17% decrease in magnitude of RMS tractions with HUVEC treated with D-mannitol and a 5% and 10% decrease in magnitude of RMS tractions with HUVEC with a high glucose treatment when compared to HUVEC with normal glucose at 0 hours and 3 hours of experiments.

## CONCLUSION

This project pushes the boundaries of utilizing mechanical engineering principles to study how hyperglycemia affects the endothelial biomechanical response in-vitro. Since there is limited data on this topic area, this project was conducted to advance our understanding of glucose-induced cell dysfunctions by showing how mechanotransduction is affected in a static hyperglycemic microenvironment.

For this study, we cultured HUVEC monolayers in three glucose conditions: normal glucose (4 mmol/l of D-glucose), high glucose (30mmol/l of D-glucose), and an osmotic control (4 mmol/l of D-glucose + 26 mmol/l of D-mannitol). We calculated the cell-to-substrate tractions and cell-cell intercellular stresses utilizing traction force microscopy and monolayer stress microscopy, respectively. Our results show that hyperglycemia and osmotic control conditions yielded a decreased response of RMS tractions, average normal stresses, and maximum shear stresses compared to normal glucose HUVEC monolayers.

We hypothesize that the osmotic control induced by high glucose plays a role in the endothelium's ability to generate tractions and intercellular stresses. Decreased tractions and intercellular stresses may influence the endothelial's ability to perform vital functions such as regulating vascular tone. This could lead to the progression and development of endothelial dysfunctions. With hyperglycemia affecting both the endothelial's molecular and mechanical mechanisms, the likelihood of inflammation, increased permeability, slower wound healing, and increased apoptosis is increased. Hyperglycemia affects endothelial cells both physically and molecularly. Taken all the factors together, we present this report on the endothelial

biomechanical response under the influence of different levels of glucose. We believe our results can lead to an increased understanding of vascular biology and aid in further research on new therapies and techniques.

The broader impact of my work can be seen in the ways it utilizes mechanical engineering applications in biology and medicine. Studying cellular mechanics has a significant societal impact since it will help researchers understand how cells sense and respond to their mechanical environments. With this new perspective, scientists and researchers will be able to consider newly discovered mechanisms and design effective treatments that can function equally in healthy and diseased environments. My work has the potential to fundamentally increase our understanding of the correlation between diabetes, the endothelium, and cardiovascular diseases and pave the way for new targeted, personalized therapies.

## REFERENCES

- [1] Centers for Disease Control and Prevention. (2022, January 18). *National Diabetes Statistics Report*. Centers for Disease Control and Prevention. Retrieved July 30, 2022, from <https://www.cdc.gov/diabetes/data/statistics-report/index.html>
- [2] Cardiovascular Disease | ADA. (2022). Retrieved July 30, 2022, from <https://www.diabetes.org/diabetes/cardiovascular-disease>
- [3] Mayo Foundation for Medical Education and Research. (2020, June 27). *Hyperglycemia in diabetes*. Mayo Clinic. Retrieved July 30, 2022, from <https://www.mayoclinic.org/diseases-conditions/hyperglycemia/symptoms-causes/syc-20373631>
- [4] Adeyinka, A., & Kondamudi, N. P. (2022, May 22). *Hyperosmolar Hyperglycemic Syndrome*. National Library of Medicine. Retrieved July 30, 2022, from <https://www.ncbi.nlm.nih.gov/books/NBK482142/>
- [5] Mayo Foundation for Medical Education and Research. (2020, July 25). *Diabetic Hyperosmolar Syndrome*. Mayo Clinic. Retrieved July 30, 2022, from <https://www.mayoclinic.org/diseases-conditions/diabetic-hyperosmolar-syndrome/symptoms-causes/syc-20371501>
- [6] Jackson, E. K. (2014, November 28). *Renal Pharmacology*. Reference Module in Biomedical Sciences. Retrieved July 30, 2022, from <https://www.sciencedirect.com/science/article/pii/B9780128012383002476>
- [7] Funk, S. D., Yurdagul, A., & Orr, A. W. (2012, February 14). *Hyperglycemia and endothelial dysfunction in atherosclerosis: Lessons from type 1 diabetes*. International Journal of Vascular Medicine. Retrieved July 30, 2022, from <https://www.hindawi.com/journals/ijvm/2012/569654/>
- [8] Kolluru, GK (2012, February 12). *Endothelial dysfunction and diabetes: Effects on angiogenesis, vascular remodeling, and wound healing*. International journal of vascular medicine. Retrieved July 30, 2022, from <https://pubmed.ncbi.nlm.nih.gov/22611498/>
- [9] H, Cai. (2000, November 10). *Endothelial dysfunction in cardiovascular diseases: The role of Oxidant Stress*. Circulation research. Retrieved July 30, 2022, from <https://pubmed.ncbi.nlm.nih.gov/11073878/>
- [10] RA, H. M. Z. W. W. J. T. D. (2014, July 15). *Disruption of endothelial adherens junctions by high glucose is mediated by protein kinase C- $\beta$ -dependent vascular endothelial cadherin tyrosine phosphorylation*. Cardiovascular diabetology. Retrieved July 30, 2022, from <https://pubmed.ncbi.nlm.nih.gov/25927959/>

- [11] Furchgott, R. F. (n.d.). *Role of endothelium in responses of vascular smooth muscle*. Circulation research. Retrieved July 30, 2022, from <https://pubmed.ncbi.nlm.nih.gov/6313250/>
- [12] Gimbrone, M. A. (n.d.). *Interactions of platelets and leukocytes with vascular endothelium: In vitro studies*. Annals of the New York Academy of Sciences. Retrieved July 30, 2022, from <https://pubmed.ncbi.nlm.nih.gov/6820246/>
- [13] Li, J., & Chen, J. (2007). *Pathophysiology of acute wound healing*. Clinics in dermatology. Retrieved July 30, 2022, from <https://pubmed.ncbi.nlm.nih.gov/17276196/>
- [14] Harrison, D. G. (1997, November 1). *Cellular and molecular mechanisms of endothelial cell dysfunction*. The Journal of clinical investigation. Retrieved July 30, 2022, from <https://pubmed.ncbi.nlm.nih.gov/9410891/>
- [15] Hamuro, M., Polan, J., & Natarajan, M. (2002, June). *High glucose induced nuclear factor kappa B mediated inhibition of endothelial cell migration*. Atherosclerosis. Retrieved July 30, 2022, from <https://pubmed.ncbi.nlm.nih.gov/11996947/>
- [16] Curcio, F., & Ceriello, A. (1992). *Decreased cultured endothelial cell proliferation in high glucose medium is reversed by antioxidants: New insights on the pathophysiological mechanisms of diabetic vascular complications*. In vitro cellular & developmental biology: journal of the Tissue Culture Association. Retrieved July 30, 2022, from <https://pubmed.ncbi.nlm.nih.gov/1483970/>
- [17] *Endothelial*. Endothelial | Cell Applications. (n.d.). Retrieved July 30, 2022, from <https://www.cellapplications.com/endothelial>
- [18] Steward, R., Tambe, D., Hardin, C. C., Krishnan, R., & Fredberg, J. J. (2015, April 15). *Fluid shear, intercellular stress, and Endothelial Cell Alignment*. American journal of physiology. Cell physiology. Retrieved July 30, 2022, from <https://www.ncbi.nlm.nih.gov/pmc/articles/PMC4398851/>
- [19] Trepap, X., Wasserman, M. R., Angelini, T. E., Millet, E., Weitz, D. A., Butler, J. P., & Fredberg, J. J. (2009, May 3). *Physical forces during collective cell migration*. Nature News. Retrieved July 30, 2022, from <https://www.nature.com/articles/nphys1269>
- [20] Ulfhammer, E. (n.d.). *Impairment of endothelial thromboprotective function by haemodynamic ...* Research Gate. Retrieved July 30, 2022, from [https://www.researchgate.net/profile/Erik-Ulfhammer/publication/228557921\\_Impairment\\_of\\_Endothelial\\_Thromboprotective\\_Function\\_by\\_Haemodynamic\\_and\\_Inflammatory\\_Stress-Implications\\_for\\_hypertensive\\_disease/links/02bfe513ed73c33482000000/Impairment](https://www.researchgate.net/profile/Erik-Ulfhammer/publication/228557921_Impairment_of_Endothelial_Thromboprotective_Function_by_Haemodynamic_and_Inflammatory_Stress-Implications_for_hypertensive_disease/links/02bfe513ed73c33482000000/Impairment)



-of-Endothelial-Thromboprotective-Function-by-Haemodynamic-and-Inflammatory-Stress-Implications-for-hypertensive-disease.pdf?origin=publication\_detail